GaSb-based SESAM mode-locked Tm:YAG ceramic laser at 2 µm

Alexander Gluth,[1] Yicheng Wang,[1] Valentin Petrov,[1] Jonna Paajaste,[2] Soile Suomalainen,[2] Antti Härkönen,[2] Mircea Guina,[2] Günter Steinmeyer,[1,2] Xavier Mateos,[3] Stefano Veronesi,[4] Mauro Tonelli,[4] Jiang Li,[5] Yubai Pan,[5] Jingkun Guo,[5] and Uwe Griebner[1,*]

[1]*Max Born Institute for Nonlinear Optics and Short Pulse Spectroscopy, Max-Born-Str. 2a, 12489 Berlin, Germany*
[2]*Optoelectronics Research Centre, Tampere University of Technology, P.O. Box 692, FIN-33101 Tampere, Finland*
[3]*Física i Cristal·lografia de Materials i Nanomaterials, Universitat Rovira i Virgili Tarragona, Campus Sescelades, c/ Marcel.lí Domingo, s/n, 43007-Tarragona, Spain*
[4]*NEST Istituto Nanoscienze-CNR and Dipartimento di Fisica dell'Università di Pisa, Largo B. Pontecorvo 3, 56127 Pisa, Italy*
[5]*Key Laboratory of Transparent Opto-functional Inorganic Materials, Shanghai Institute of Ceramics, Chinese Academy of Sciences, Shanghai 200050, China*
**griebner@mbi-berlin.de*

Abstract: Tunable and mode-locked laser operation near 2 µm based on different Tm-doped YAG ceramics, 4 at.% and 10 at.%, is demonstrated. Several designs of GaSb-based surface-quantum-well SESAMs are characterized and studied as saturable absorbers for mode-locking. Best mode-locking performance was achieved using an antireflection-coated near-surface quantum-well SESAM, resulting in a pulse duration of ~3 ps and ~150 mW average output power at 89 MHz. All mode-locked Tm:YAG ceramic lasers operated at 2012 nm, with over 133 nm demonstrated tuning for continuous-wave operation.

OCIS codes: (140.4050) Mode-locked lasers; (140.3070) Infrared and far-infrared lasers.

References and links

1. M. Ebrahim-Zadeh and I. T. Sorokina, eds., *Mid-infrared Coherent Sources and Applications* (Springer, 2008).
2. R. R. Gattass and E. Mazur, "Femtosecond laser micromachining in transparent materials," Nat. Photonics **2**(4), 219–225 (2008).
3. R. Targ, B. C. Steakley, J. G. Hawley, L. L. Ames, P. Forney, D. Swanson, R. Stone, R. G. Otto, V. Zarifis, P. Brockman, R. S. Calloway, S. H. Klein, and P. A. Robinson, "Coherent lidar airborne wind sensor II: flight-test results at 2 and 10 vm," Appl. Opt. **35**(36), 7117–7127 (1996).
4. F. Dausinger, F. Lichtner, and H. Lubatschowski, *Femtosecond Technology for Technical and Medical Applications* (Springer, 2004).
5. M. Eichhorn, "Quasi-three-level solid-state lasers in the near and mid infrared based on trivalent rare earth ions," Appl. Phys. B **93**(2-3), 269–316 (2008).
6. N. Coluccelli, G. Galzerano, D. Gatti, A. Di Lieto, M. Tonelli, and P. Laporta, "Passive mode-locking of a diode-pumped Tm:$GdLiF_4$ laser," Appl. Phys. B **101**(1-2), 75–78 (2010).
7. A. A. Lagatsky, S. Calvez, J. A. Gupta, V. E. Kisel, N. V. Kuleshov, C. T. A. Brown, M. D. Dawson, and W. Sibbett, "Broadly tunable femtosecond mode-locking in a Tm:KYW laser near 2 µm," Opt. Express **19**(10), 9995–10000 (2011).
8. A. A. Lagatsky, F. Fusari, S. Calvez, S. V. Kurilchik, V. E. Kisel, N. V. Kuleshov, M. D. Dawson, C. T. A. Brown, and W. Sibbett, "Femtosecond pulse operation of a Tm,Ho-codoped crystalline laser near 2 microm," Opt. Lett. **35**(2), 172–174 (2010).
9. A. A. Lagatsky, X. Han, M. D. Serrano, C. Cascales, C. Zaldo, S. Calvez, M. D. Dawson, J. A. Gupta, C. T. A. Brown, and W. Sibbett, "Femtosecond (191 fs) $NaY(WO_4)_2$ Tm,Ho-codoped laser at 2060 nm," Opt. Lett. **35**(18), 3027–3029 (2010).
10. K. Yang, D. Heinecke, J. Paajaste, C. Kölbl, T. Dekorsy, S. Suomalainen, and M. Guina, "Mode-locking of 2 µm Tm,Ho:YAG laser with GaInAs and GaSb-based SESAMs," Opt. Express **21**(4), 4311–4318 (2013).
11. K. J. Yang, D. C. Heinecke, C. Kölbl, T. Dekorsy, S. Z. Zhao, L. H. Zheng, J. Xu, and G. J. Zhao, "Mode-locked Tm,Ho:YAP laser around 2.1 µm," Opt. Express **21**(2), 1574–1580 (2013).

#226418 - $15.00 USD Received 6 Nov 2014; revised 19 Dec 2014; accepted 19 Dec 2014; published 20 Jan 2015

12. N. Coluccelli, A. A. Lagatsky, A. Di Lieto, M. Tonelli, G. Galzerano, W. Sibbett, and P. Laporta, "Passive mode locking of an in-band-pumped Ho:$YLiF_4$ laser at 2.06 μm," Opt. Lett. **36**(16), 3209–3211 (2011).
13. A. Härkönen, C. Grebing, J. Paajaste, R. Koskinen, J.-P. Alanko, S. Suomalainen, G. Steinmeyer, and M. Guina, "Modelocked GaSb disk laser producing 384 fs pulses at 2 µm wavelength," Electron. Lett. **47**(7), 454 (2011).
14. M. Guina, A. Härkönen, V.-M. Korpijärvi, T. Leinonen, and S. Suomalainen, "Semiconductor Disk Lasers: Recent Advances in Generation of Yellow-Orange and Mid-IR Radiation," Adv. Opt. Technol. **2012**, 1–19 (2012).
15. U. Keller, "Recent developments in compact ultrafast lasers," Nature **424**(6950), 831–838 (2003).
16. A. Schmidt, P. Koopmann, G. Huber, P. Fuhrberg, S. Y. Choi, D.-II. Yeom, F. Rotermund, V. Petrov, and U. Griebner, "175 fs Tm:Lu_2O_3 laser at 2.07 µm mode-locked using single-walled carbon nanotubes," Opt. Express **20**, 5313–5318 (2012).
17. J. Liu, Y. Wang, Z. Qu, and X. Fan, "2µm passive Q-switched mode-locked Tm^{3+}:YAP laser with single-walled carbon nanotube absorber," Opt. Laser Technol. **44**(4), 960–962 (2012).
18. A. Schmidt, S. Y. Choi, D. Yeom, F. Rotermund, X. Mateos, M. Segura, F. Díaz, V. Petrov, and U. Griebner, "Femtosecond pulses near 2 µm from a Tm:KLuW laser mode-locked by a single-walled carbon nanotube saturable absorber," Appl. Phys. Express **5**(9), 092704 (2012).
19. J. Ma, G. Xie, P. Lv, W. Gao, P. Yuan, L. Qian, U. Griebner, V. Petrov, H. Yu, H. Zhang, and J. Wang, "Wavelength-versatile graphene-gold film saturable absorber mirror for ultra-broadband mode-locking of bulk lasers," Scientific Reports. **4,** 5016, 1–6 (2014).
20. A. A. Lagatsky, Z. Sun, T. S. Kulmala, R. S. Sundaram, S. Milana, F. Torrisi, O. L. Antipov, Y. Lee, J. H. Ahn, C. T. A. Brown, W. Sibbett, and A. C. Ferrari, "2 µm solid-state laser mode-locked by single-layer graphene," Appl. Phys. Lett. **102**(1), 013113 (2013).
21. R. C. Stoneman and L. Esterowitz, "Efficient, broadly tunable, laser-pumped Tm:YAG and Tm:YSGG CW lasers," Opt. Lett. **15**(9), 486–488 (1990).
22. T. Yokozawa and H. Hara, "Laser-diode end-pumped Tm(3+):YAG eye-safe laser," Appl. Opt. **35**(9), 1424–1426 (1996).
23. C. Li, J. Song, D. Shen, N. S. Kim, K. Ueda, Y. Huo, S. He, and Y. Cao, "Diode-pumped high-efficiency Tm:YAG lasers," Opt. Express **4**(1), 12–18 (1999).
24. Y. F. Li, Y. Z. Wang, and Y. L. Ju, "Comparative study of LD-Pumped Tm:YAG and Tm:LuAG lasers," Laser Phys. **18**(6), 722–724 (2008).
25. J. F. Pinto, L. Esterowitz, and G. H. Rosenblatt, "Continuous-wave mode-locked 2- microm Tm: YAG laser," Opt. Lett. **17**(10), 731–732 (1992).
26. A. Ikesue, K. Kamata, and K. Yoshida, "Synthesis of Nd^{3+}, Cr^{3+}-codoped YAG ceramics for high-efficiency solid-state lasers," J. Am. Ceram. Soc. **78**(9), 2545–2547 (1995).
27. W.-X. Zhang, Y.-B. Pan, J. Zhou, W.-B. Liu, J. Li, B.-X. Jiang, X.-J. Cheng, and J.-Q. Xu, "Diode-pumped Tm:YAG ceramic laser," J. Am. Ceram. Soc. **92**(10), 2434–2437 (2009).
28. W.-X. Zhang, Y.-B. Pan, J. Zhou, W.-B. Liu, J. Li, Y.-W. Zou, and Z.-Y. Wei, "Preparation and characterization of transparent Tm:YAG ceramics," Ceram. Int. **37**(3), 1133–1137 (2011).
29. Q.-L. Ma, Y. Bo, N. Zong, Y.-B. Pan, Q.-J. Peng, D.-F. Cui, and Z.-Y. Xu, "Light scattering and 2-µm laser performance of Tm:YAG ceramic," Opt. Commun. **284**(6), 1645–1647 (2011).
30. S. Zhang, X. Wang, W. Kong, Q. Yang, J. Xu, B. Jiang, and Y. Pan, "Efficient Q-switched Tm:YAG ceramic slab laser pumped by a 792 nm fiber laser," Opt. Commun. **286**, 288–290 (2013).
31. Y. Zou, Z. Wei, Q. Wang, M. Zhan, D. Li, Z. Zhang, J. Zhang, and D. Tang, "High-efficiency diode-pumped Tm:YAG ceramic laser," Opt. Mater. **35**(4), 804–806 (2013).
32. J. T. Thomas, M. Tonelli, S. Veronesi, E. Cavalli, X. Mateos, V. Petrov, U. Griebner, J. Li, Y. Pan, and J. Guo, "Optical spectroscopy of Tm $^{3+}$:YAG transparent ceramics," J. Phys. D Appl. Phys. **46**(37), 375301 (2013).
33. A. A. Lagatsky, O. L. Antipov, and W. Sibbett, "Broadly tunable femtosecond Tm:Lu_2O_3 ceramic laser operating around 2070 nm," Opt. Express **20**(17), 19349–19354 (2012).
34. U. Keller, T. H. Chiu, and J. F. Ferguson, "Self-starting femtosecond mode-locked Nd:glass laser that uses intracavity saturable absorbers," Opt. Lett. **18**(13), 1077 (1993).
35. Y. Silberberg, P. W. Smith, D. A. B. Miller, B. Tell, A. C. Gossard, and W. Wiegmann, "Fast nonlinear optical response from proton-bombarded multiple quantum well structures," Appl. Phys. Lett. **46**(8), 701–703 (1985).
36. A. Garnache, B. Sermage, R. Teissier, G. Saint-Giro, and I. Sagnes, "A new kind of fast quantum-well semiconductor saturable-absorber mirror with low losses for ps pulse generation," International Conference on Indium Phosphide and Related Materials, May 2003, pp. 247–250 (2003).
37. F. Saas, G. Steinmeyer, U. Griebner, M. Zorn, and M. Weyers, "Exciton resonance tuning for the generation of sub-picosecond pulses from a mode-locked semiconductor disk laser," Appl. Phys. Lett. **89**(14), 141107 (2006).
38. H. K. Choi, G. W. Turner, and S. J. Eglash, "High-power GaInAsSb-AlGaAsSb diode lasers emitting at 1.9 µm," IEEE Photon. Technol. Lett. **6**, 7–9 (1994).
39. C. Lin, M. Grau, O. Dier, and M. C. Amann, "Low-threshold room-temperature cw operation of 2.24–3.04 µm GaInAsSb/AlGaAsSb quantum-well lasers," Appl. Phys. Lett. **84**(25), 5088–5090 (2004).
40. J. Paajaste, S. Suomalainen, R. Koskinen, A. Härkönen, G. Steinmeyer, and M. Guina, "GaSb-based semiconductor saturable absorber mirrors for mode-locking 2 µm semiconductor disk lasers," Phys. Stat. Solid. C. **9**(2), 294–297 (2012).

#226418 - $15.00 USD Received 6 Nov 2014; revised 19 Dec 2014; accepted 19 Dec 2014; published 20 Jan 2015

41. J. Paajaste, S. Suomalainen, A. Härkönen, U. Griebner, G. Steinmeyer, and M. Guina, "Absorption recovery dynamics in 2 µm GaSb-based SESAMs," J. Phys. D **46**, 065102 (2014).
42. J. Li, J. Zhou, Y. B. Pan, W. B. Liu, W. X. Zhang, J. K. Guo, H. Chen, D. Y. Shen, X. F. Yang, and T. Zhao, "Solid-state reactive sintering and optical characteristics of transparent Er:YAG laser ceramics," J. Am. Ceram. Soc. **95**, 1029–1032 (2012).
43. P. Song, Z. Zhao, X. Xu, B. Jang, P. Deng, and J. Xu, "Growth and properties of Tm: YAG crystals," J. Cryst. Growth **270**(3-4), 433–437 (2004).
44. S. A. Payne, L. L. Chase, L. K. Smith, W. L. Kway, and W. F. Krupke, "Infrared cross-section measurements for crystals doped with Er^{3+}, Tm^{3+}, and Ho^{3+}," IEEE J. Quantum Electron. **28**(11), 2619–2630 (1992).
45. R. Fehse, S. Tomic, A. R. Adams, S. J. Sweeney, E. P. O'Reilly, A. Andreev, and H. Riechert, "A quantitative study of radiative, Auger, and defect related recombination processes in 1.3-µm GaInNAs-based quantum-well lasers," IEEE J. Sel. Top. Quantum Electron. **8**(4), 801–810 (2002).
46. A. Jasik, J. Muszalski, K. Hejduk, and M. Kosmala, "The reduced temporal parameters of passivated semiconductor saturable absorber mirror," Thin Solid Films **518**(1), 171–173 (2009).

1. Introduction

Ultrashort pulse laser sources at 2 µm are of growing interest for the use as pump and seed sources in optical parametric systems operating in the mid-IR, for IR supercontinuum generation, and for time-resolved spectroscopy [1–4].

The most popular lasers operating around 2 µm, both in continuous wave and pulsed mode, are based on the trivalent Tm and Ho ions [5]. Typically, femto- and picosecond lasers operating around 2 µm are passively mode-locked, using different types of saturable absorbers. Using bulk laser media and semiconductor saturable absorber mirrors (SESAM) [15], ultrashort pulse generation near 2 µm was demonstrated for Tm and Ho doped lasers, including co-doped variants [6–12]. Similarly, mode-locked semiconductor disk lasers were demonstrated in this wavelength range [13, 14]. Single-walled carbon nanotubes [16–18] and graphene [19, 20] were also used as passive mode-lockers at 2 µm, however, so far only for Tm-doped crystals. In particular, the Tm:YAG single crystal is a well established 2 µm laser medium and has been investigated in detail, leading to exceptional continuous-wave (CW) and Q-switched laser performance [21–24]. Nevertheless, despite more than two decades of efforts, mode-locked Tm:YAG lasers have only been demonstrated with active mode-locking, generating pulse durations of 35 ps at 2.01 µm [25]. The excellent thermal properties of the crystalline host therefore come at the expense of a fairly limited picosecond performance so far. To this end, laser ceramics appear an intriguing alternative, combining good thermal properties with potentially less restrictive bandwidth limitations than crystalline hosts.

Ceramics come with a number of beneficial properties. First, fabrication of ceramic materials is generally less complex than single-crystal growth, in particular when it comes to large dimensions. Furthermore, higher doping concentrations with uniform distribution as well as simplified shaping and processing are achievable [26]. Unfortunately only very few materials, such as YAG and some of the cubic sesquioxides, can currently be manufactured as ceramics.

Given the potential of the laser ceramics, efforts have focused on the realization of high quality Tm^{3+}:YAG ceramics. Originally, the sintering process for the fabrication of Tm:YAG transparent ceramics was reported by Zhang *et al*. [27, 28]. During the last three years, their diode-pumped CW laser performance was significantly improved, and output powers of several watts were obtained, with slope efficiencies exceeding 40% [29–31]. Spectroscopic properties of transparent Tm:YAG ceramics, including absorption, emission, and fluorescence decay times have been thoroughly investigated [32]. Besides YAG, sesquioxide-based ceramics were studied, too. Very recently SESAM mode-locked laser operation was reported for a Tm:Lu_2O_3 ceramic laser delivering 180 fs pulses [33].

Mode-locking of 2 µm lasers strongly relies on available saturable absorber technology in this range. One specific concern is the relaxation time of the saturable absorber, which indirectly limits the obtainable pulse duration. For nearly defect-free GaAs- and InP-based SESAMs, e.g., this time constant typically amounts to tens or hundreds of picoseconds. Therefore, advanced growth and post-processing techniques, such as low-temperature growth

#226418 - $15.00 USD Received 6 Nov 2014; revised 19 Dec 2014; accepted 19 Dec 2014; published 20 Jan 2015

[34], ions irradiation/implantation [35], or surface quantum wells (QWs) [36, 37] have to be applied for accelerating the absorption recovery of near-infrared SESAMs. In the mid-IR, GaSb offers a viable alternative to the previously discussed material systems. This technology employs lattice-matched GaSb/AlAsSb distributed Bragg reflectors (DBRs), which enable a very broad reflection band of about 300 nm. Moreover, band gap and offset in GaInAsSb/AlGaAsSb QWs can be tailored to cover emission in a wavelength range from 1.9 µm [38] to beyond 3 µm [39]. In mode-locked bulk laser experiments at 2 µm wavelength, recovery of the employed GaSb-based SESAMs was accelerated by irradiating the quantum wells with As^+ ions [7–9, 12, 33]. Recent studies suggest that the absorption recovery time is rather independent of growth temperature or strain in the QWs [40, 41]. The surprisingly fast absorption recovery time for these low-defect hetero-structures was attributed to the fact that in narrow band gap materials, such as GaSb compounds, the Auger recombination is significantly stronger than in GaAs and InP heterostructures [40].

Here we report passive mode-locking of different Tm:YAG transparent ceramics employing novel near-surface GaSb-based SESAMs, setting a new record pulse duration for this intriguing laser material. Most of this improvement is due to the development of a new SESAM technology, which allows obtaining fast carrier relaxation without introduction of additional non-saturable losses at this challenging wavelength.

2. Tm:YAG ceramics and GaSb-based SESAMs

We investigated two transparent YAG ceramics, doped with 4 and 10 at.% Tm^{3+}. These samples were fabricated by solid-state reactive sintering of commercial α-Al_2O_3, Y_2O_3 and Tm_2O_3 powders with purity higher than 99.99%, using MgO powder and tetraethoxysilane (TEOS) to favor the sintering process, i.e., very similar to our previous fabrication methodology [42]. Both ceramic samples are 3.4 mm thick with an aperture of 3.2 × 3.2 mm^2.

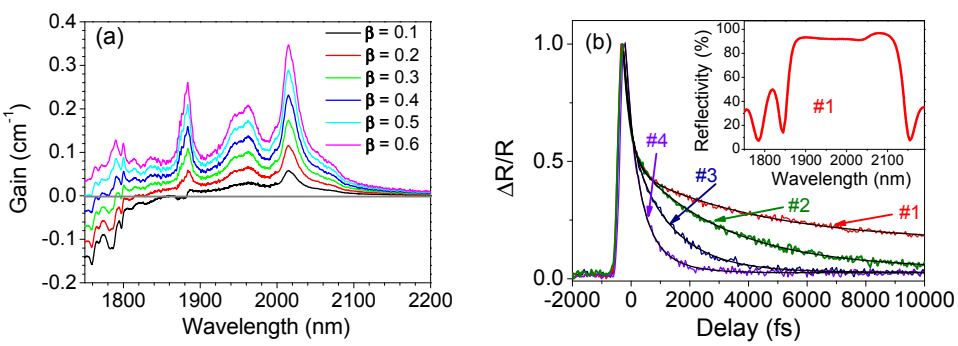

Fig. 1. (a) Gain of the 4 at.% Tm:YAG ceramic for different inversion levels β ($\sigma_{gain} = \beta\sigma_{em} - (1 - \beta)\sigma_{abs}$). (b) Pump-probe traces (colored) and bi-exponential fits to the data (black) of the four studied AR-coated QW SESAMs recorded at 2.0 µm (ΔR/R – reflectivity change). The inset shows the measured reflectivity of SESAM #1 (error margin of the microfocus measurement: 2%). For SESAM-designs, see Table 1.

The maximum absorption cross section σ_{abs} is located at 786 nm and amounts to 0.76 × 10^{-20} cm^2. The maximum emission cross section σ_{em} for the $^3F_4 \rightarrow {}^3H_6$ Tm^{3+} laser transition at 2014 nm is 0.30 × 10^{-20} cm^2 [32]. These values are slightly higher compared to Tm:YAG single crystals: σ_{abs} = 0.63 × 10^{-20} cm^2 [43] and σ_{em} = 0.22 × 10^{-20} cm^2 [44]. The gain curves for the 4 at% Tm:YAG ceramic are shown in Fig. 1(a) for different inversion levels β. The decay time of the $^3F_4$ emission for the 4 at.% Tm:YAG ceramic was determined as 10 ms at room temperature [32], which is in good agreement with the value reported for single crystals [44].

#226418 - $15.00 USD Received 6 Nov 2014; revised 19 Dec 2014; accepted 19 Dec 2014; published 20 Jan 2015

Based on a recent study [41], we concluded that near-surface placement of the QWs and additional anti-reflection (AR) coating may hold a rather unique opportunity for tailoring the recovery time of a GaSb-based SESAM. In turn, slightly modifying its structure, we developed a suitable SESAM for passive mode-locking of Tm:YAG ceramics. These GaSb-based SESAMs were grown at a temperature of 350°C using conventional solid-source molecular beam epitaxy. First, a GaSb-buffer was grown on a (100) n-GaSb substrate followed by a lattice-matched AlAsSb/GaSb DBR consisting of 18.5 layer pairs. The absorber region is anti-resonant at the operating wavelength of 2 μm and consists of 10-nm thick InGaAsSb QWs embedded in GaSb. Sample #2 contained two QWs separated by a 10 nm GaSb barrier with a cap having a thickness of 5 nm. Sample #3 included a single QW with a GaSb cap thickness of 5 nm. Sample #4 also featured a single QW, however, the cap thickness was adjusted to 10 nm. Sample #1 had three QWs, however placed in an area 300 nm below the surface. Finally, an AR coating was deposited on all samples. This coating consists of a dielectric two-layer (TiO_2/SiO_2) structure. The AR coating increases the modulation contrast and reduces the saturation energy, but at the same time, it decreases the recovery time. This intriguing effect was attributed to increased Auger recombination, owing to enhancement of the interaction between the optical field and the near-surface QW [41]. Here it is important to understand that the Auger recombination rate is proportional to the cube of the carrier density [45]. Note also that dielectric coatings are often exploited for surface passivation of semiconductor samples [46]. This aspect becomes particularly important for GaSb interfaces, which oxidize very fast. The reflectivity graph of SESAM #1 is shown in the inset of Fig. 1(b). Taking into account the error margin of the microfocus reflectivity measurement of 2% and the deduced peak absorption of ~1.5% per QW the insertion loss at the lasing wavelength of 2.01 μm is roughly 3% to 6% depending on the number of QWs in the samples.

To investigate the absorption recovery dynamics, pump-probe measurements using the idler wave at 2.0 μm of an optical parametric oscillator (OPO) were performed. The OPO (Opal, Spectra Physics) delivers about 130 mW average power at 80 MHz repetition rate, 150 fs pulse duration, and nearly 2 nJ pulse energy resulting in an averaged pump pulse fluence of ~50 μJ/cm^2. The results are shown in Fig. 1(b). For all samples, the intraband relaxation times τ_1 (fast component) behave very similarly and amount to <0.5 ps. Similar to near-IR SESAMs, this component typically has little weight and does not dominate the pulse shaping process. In contrast, the interband relaxation time τ_2 (slow component) for the SESAMs with the QWs placed 10 nm beneath the surface is shorter than 5 ps and appears slightly decreased compared to those with >5 times thicker cap layers. This reduction is explained by fast recombination via surface states. In SESAM #2 employing two QWs, the reduction of τ_2 due to surface recombination is not as pronounced as in the SESAMs #3 and #4 since the second QW is further away from the surface. Extremely low τ_2 values of ~1.7 ps have been found for the samples incorporating one QW and a cap layer thickness ≤10 nm.

3. Laser setup and continuous-wave Tm:YAG ceramic laser

All laser experiments were performed in a X-shaped astigmatically compensated linear cavity in which the Tm:YAG ceramics were positioned at Brewster angle in the central folding (Fig. 2). A CW Ti:sapphire laser served as the pump source with a few watts available power at the absorption maximum. The pump laser was focused to a waist radius of ~30 μm. Here the curved mirror M4 acts as a back-reflector for the unabsorbed pump. Under lasing conditions for double–pass pumping, the 4 and 10 at.% TmYAG ceramics absorbed about 75% and 95% of the incident pump power, respectively.

#226418 - $15.00 USD Received 6 Nov 2014; revised 19 Dec 2014; accepted 19 Dec 2014; published 20 Jan 2015

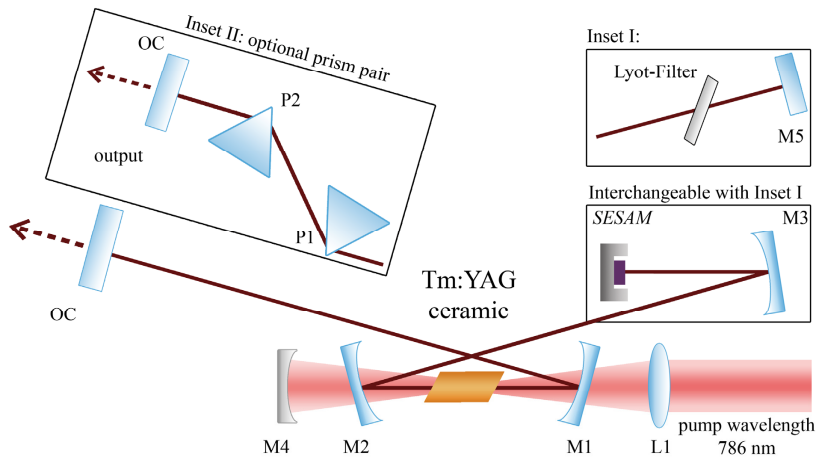

Fig. 2. Setup of the Tm:YAG ceramic laser. L1: focusing lens; M1, M2 and M3: concave mirrors with radius of curvature (RoC) = 100 mm; M4 curved pump mirror, RoC = 100 mm; M5 plane HR-mirror; P1, P2: CaF_2 prisms; OC: output coupler. Insets: exchanging parts for tunable CW operation (Birefringent (Lyot)-Filter) or dispersion compensation line (prisms).

Initially, CW laser operation was studied using a plane HR end mirror (M5) and without any prisms intracavity. Figure 3(a) shows the CW laser performance of the two ceramics for 3% output coupler transmission (T_{oc}). Slope efficiencies are very similar and amount to 42.5% and 44.7% for the 4 and 10 at.% Tm-doped ceramics, respectively. The maximum output power achieved was slightly higher for the 10 at.% sample (1.1 W) compared to 4 at.% (0.9 W), which is due to the lower pump power absorption of the latter. Using T_{oc} = 5% the maximum CW output power was the same as with T_{oc} = 3%, however the slope efficiencies were slightly improved and amounted to 48% and 50% for the 4 and 10 at.% Tm-doped ceramics, respectively.

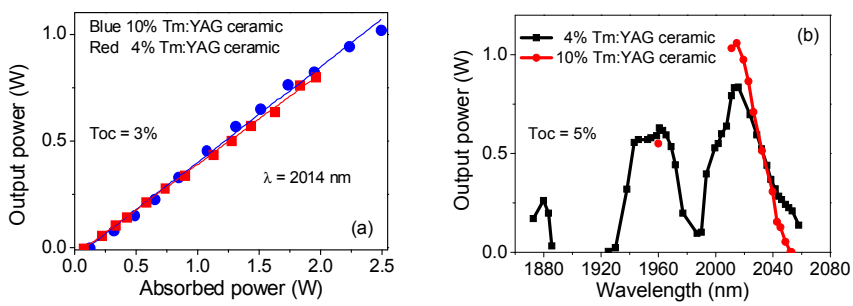

Fig. 3. CW laser performance of the 4 and 10 at.% Tm:YAG ceramic lasers: (a) output power vs. absorbed pump power and linear fits for the slope efficiencies. (b) Spectral tunability for an incident pump power of 2.5 W.

Spectral tunability was investigated by inserting a 3-mm thick single-stage birefringent filter. Figure 3(b) depicts the results achieved with T_{oc} = 5%. For the 4 at.% ceramic, a continuous tuning range from 1925 to 2058 nm was obtained. These tuning curve shows a pronounced structure, which is in accordance with the gain curve, cf. Figure 1(a). Additionally, lasing was also observed in a separate narrow spectral window at about 1880 nm, Fig. 3(b). In contrast, using the 10 at.%-doped Tm:YAG in the cavity, CW tuning was only achieved between 2010 and 2055 nm as well as at a solitary lasing point at 1960 nm. The latter coincides with a local gain maximum, cf. Figure 1(a). We attribute the limited tunability below 2010 nm to the higher Tm-doping level (2.5 times). Higher doping typically shifts the

#226418 - $15.00 USD Received 6 Nov 2014; revised 19 Dec 2014; accepted 19 Dec 2014; published 20 Jan 2015

emission to longer wavelengths due to higher reabsorption. Under similar pump conditions for the two Tm:YAG ceramics, as in our case, the inversion parameter β, cf. Figure 1(a), is lower for the 10 at.% Tm-doped sample, resulting in a narrower spectral tuning range. For the 4 at.% Tm:YAG ceramic, the CW tuning range of 133 nm (T_{oc} = 5%) is comparable to that demonstrated with Tm:YAG single crystals of ~150 nm, however, with lower output coupling (T_{oc} = 2.5%) [21].

4. SESAM mode-locked Tm:YAG ceramic laser

Mode-locking of the Tm:YAG ceramic lasers was accomplished by inserting SESAMs as end cavity reflectors in the focal region of curved mirror M3 (Fig. 2). The resulting resonator length corresponded to a repetition rate of 89 MHz. Mode-locking of both Tm:YAG ceramics was achieved with SESAMs #2, #3 and #4 (Table 1) and output coupler transmissions between 0.5% and 3%. The beam waist radius at the position of the SESAM was 30 µm, resulting in a fluence on the SESAMs of ~600 µJ/cm^2 at the mode-locking threshold. Using SESAM #1, only mode-locking with Q-switching instabilities could be observed. Given the 3-QW design of SESAM #1, a higher modulation depth results compared to the other SESAMs, which presumably gives rise to this behavior.

The performance of the 4 at.% Tm:YAG ceramic together with SESAM #4 is shown in Fig. 4(a) (T_{oc} = 1.5%). At low incident pump powers of 340 mW, i.e., 240 mW above the lasing threshold, stable and self-starting mode-locking was observed with a slope efficiency of 9.6%. The laser switched immediately from the CW-regime to stable mode-locked operation.The maximum average output power achieved for the 4 at.% Tm:YAG ceramic in the mode-locked regime amounted to 151 mW at an absorbed pump power of 1.05 W, resulting in a slope efficiency of 14% (T_{oc} = 3%).

The measured interferometric autocorrelation traces of the mode-locked 4 at.% Tm:YAG ceramic laser were similar for the three successfully operating SESAMs, and an example is shown in Fig. 4(b). From this data, the intensity autocorrelation trace was extracted by Fourier filtering, Fig. 5(a). Assuming a hyperbolic secant pulse shape, a pulse duration of 3.4 ps is then extracted from this trace. The corresponding optical spectrum, inset in Fig. 5(a), was centered at 2012 nm and displayed a FWHM of 2.7 nm. The latter supports a ~2 times shorter pulse duration, indicating slightly chirped pulses. No significant variation of the mode-locked laser performance was observed when introducing two CaF_2-prisms into the cavity. Also, when varying the output coupler transmission, the performance changed only marginally whereas the average output power increased from about 40 mW for T_{oc} = 0.5% to about 150 mW for T_{oc} = 3%. The shortest pulse duration of 2.5 ps was obtained using SESAM #4 for T_{oc} = 0.5%.

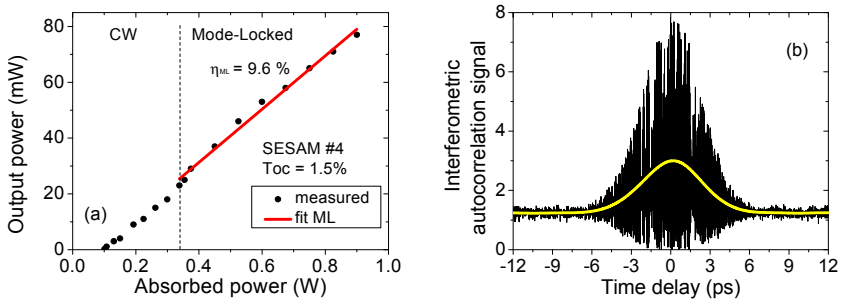

Fig. 4. Mode-locked 4 at.% Tm:YAG ceramic laser: (a) input–output characteristics (red line: slope efficiency (η) in the mode-locked regime (linear fit). (b) Measured interferometric autocorrelation signal. The measurement was based on the two-photon absorption nonlinearity in a silicon photo diode.

#226418 - $15.00 USD Received 6 Nov 2014; revised 19 Dec 2014; accepted 19 Dec 2014; published 20 Jan 2015

Application of the 10 at.% Tm:YAG ceramic in the mode-locked regime resulted in comparable pulse parameters as for the 4 at.% Tm:YAG (duration, central wavelength, bandwidth, time-bandwidth product). The extracted intensity autocorrelation trace from the two-photon absorption interferometric autocorrelation signal for the 10 at.% Tm:YAG ceramic laser mode-locked with SESAM #4 is shown in Fig. 5(b) for comparison. The higher Tm-doping only led to a reduction of the average output power by a factor of about two.

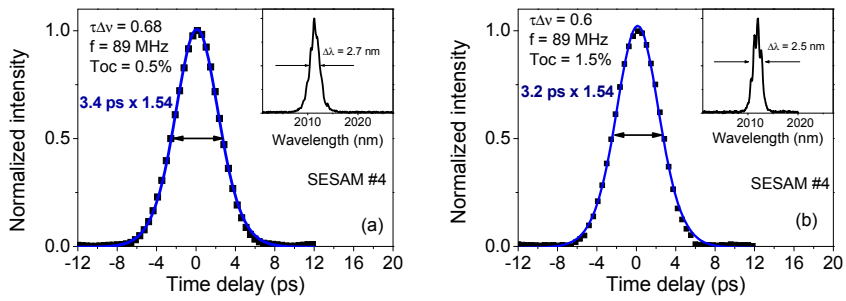

Fig. 5. Intensity autocorrelation traces extracted from the interferometric autocorrelation signals of the mode-locked Tm:YAG ceramic lasers (τΔν: time-bandwidth product). Insets: optical emission spectra: (a) 4 at.% Tm:YAG ceramic; (b) 10 at.% Tm:YAG ceramic.

The estimated overall group delay dispersion (GDD) was negative. The contribution of Tm:YAG is ~-400 fs^2 and the GDD estimated for the SESAMs is also negative and amounts to several −100 fs^2 depending on the specific SESAM design (calculated based on Fig. 1(b), inset). Note that the calculation of the SESAM GDD underlies some uncertainties related to deviations of the refractive index data in the grown structure relative to design data. Furthermore Gires-Tournois effects may contribute to the SESAM GDD, even the samples are AR-coated. Despite implementing a slightly negative overall cavity GDD, for operating the laser in the soliton-like regime, the net negative GDD seems to be too high (τΔν~0.65). This assumption is supported by the nearly unchanged pulse performance when inserting the prism pair into the cavity. The prism sequence can only deliver negative GDD of the same sign as the active material and the DBR of the SESAM near 2 µm (prism GDD in the experiments: ~-500 fs^2 to ~–3000 fs^2).

The radio-frequency (RF) spectra of the SESAM mode-locked 4 at.% Tm:YAG ceramic laser are shown in Fig. 6. Measured at a resolution bandwidth of 300 Hz, the fundamental beat note at 88.83 MHz displays a remarkably high extinction ratio of 77 dB above carrier, as shown in Fig. 6(a). As further evidence for stable CW single-pulse operation without Q-switching, Fig. 6(b) depicts a 1 GHz wide-span RF measurement.

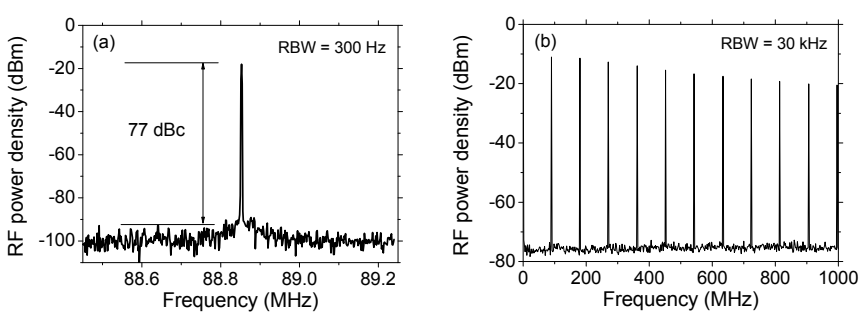

Fig. 6. Radio frequency-spectra of the SESAM mode-locked 4 at.% Tm:YAG ceramic laser: fundamental beat note (a) and 1 GHz wide-span (b). RBW: resolution bandwidth.

#226418 - $15.00 USD Received 6 Nov 2014; revised 19 Dec 2014; accepted 19 Dec 2014; published 20 Jan 2015

Table 1 lists the results obtained with both Tm:YAG ceramic lasers when using T_{oc} = 3% for all SESAMs applied. In all cases where mode-locking was achieved, a tendency toward multi-pulsing was observed. Best performance in terms of stability and output power was achieved with SESAM #2. The tendency to multi-pulse operation was stronger for the 1-QW structures (samples #3 and #4) exhibiting the lowest modulation depth. This can be explained by lower saturation energy for the 1-QW structures that favors the formation of pulses with lower energy.

Table 1. Parameters of the studied SESAMs and results with the mode-locked 4 and 10 at.%-doped Tm:YAG ceramic lasers (T_{oc} = 3%).

SESAM	No. of QWs	Cap (nm)	τ_2 (ps)	4 at.% Tm τ_p (ps)	4 at.% Tm P_{out} (mW)	10 at.% Tm τ_p (ps)	10 at.% Tm P_{out} (mW)
#1	3	300	9.7	Q-sw. instab.	Q-sw. instab.	/	/
#2	2	5	4.1	3.2	140	3.3	62
#3	1	10	1.7	3.0	135	3.3	39
#4	1	5	1.6	3.0	105	3.6	57

4. Conclusion

Tm:YAG ceramics with 4 and 10 at.%. Tm-doping were studied in different laser regimes. For the first time to our knowledge, passive mode-locking is obtained for Tm:YAG at pulse durations as short as 2.5 ps. This performance critically depends on the use of anti-reflection coated near-surface GaSb based SESAMs with recovery times <5 ps. The CW output power and the achieved mode-locked laser pulse parameters are very similar for the two Tm-dopings whereas the tuning range and the average output power in the mode-locked regime differ significantly. Best mode-locking performance was achieved by employing SESAMs with a low modulation depth, i.e., with the smallest number of quantum wells.

The presented CW spectral tuning of the 4 at.% Tm:YAG ceramic indicated at least a 40 nm bandwidth, sufficient to host pulses of sub-100 fs duration. Consequently, further experiments will be directed towards exploitation of this bandwidth potential.

Acknowledgments

This work was partially supported by National Natural Science Foundation of China (Nos. 50990301, 91022035).

#226418 - $15.00 USD Received 6 Nov 2014; revised 19 Dec 2014; accepted 19 Dec 2014; published 20 Jan 2015